



AFRL-AFOSR-JP-TR-2019-0053

---

Properties of ionic liquid ferrofluids

Brian Hawkett  
UNIVERSITY OF SYDNEY  
L 6 JFR BUILDING G02 CITY RD  
UNIVERSITY OF SYDNEY, 2006  
AU

---

09/04/2019  
Final Report

DISTRIBUTION A: Distribution approved for public release.

Air Force Research Laboratory  
Air Force Office of Scientific Research  
Asian Office of Aerospace Research and Development  
Unit 45002, APO AP 96338-5002

<b>REPORT DOCUMENTATION PAGE</b>				<i>Form Approved</i> OMB No. 0704-0188	
<p>The public reporting burden for this collection of information is estimated to average 1 hour per response, including the time for reviewing instructions, searching existing data sources, gathering and maintaining the data needed, and completing and reviewing the collection of information. Send comments regarding this burden estimate or any other aspect of this collection of information, including suggestions for reducing the burden, to Department of Defense, Executive Services, Directorate (0704-0188). Respondents should be aware that notwithstanding any other provision of law, no person shall be subject to any penalty for failing to comply with a collection of information if it does not display a currently valid OMB control number.</p> <p><b>PLEASE DO NOT RETURN YOUR FORM TO THE ABOVE ORGANIZATION.</b></p>					
<b>1. REPORT DATE (DD-MM-YYYY)</b> 04-09-2019		<b>2. REPORT TYPE</b> Final		<b>3. DATES COVERED (From - To)</b> 26 Aug 2016 to 25 Aug 2018	
<b>4. TITLE AND SUBTITLE</b> Properties of ionic liquid ferrofluids				<b>5a. CONTRACT NUMBER</b>	
				<b>5b. GRANT NUMBER</b> FA2386-16-1-4029	
				<b>5c. PROGRAM ELEMENT NUMBER</b> 61102F	
<b>6. AUTHOR(S)</b> Brian Hawkett				<b>5d. PROJECT NUMBER</b>	
				<b>5e. TASK NUMBER</b>	
				<b>5f. WORK UNIT NUMBER</b>	
<b>7. PERFORMING ORGANIZATION NAME(S) AND ADDRESS(ES)</b> UNIVERSITY OF SYDNEY L 6 JFR BUILDING G02 CITY RD UNIVERSITY OF SYDNEY, 2006 AU				<b>8. PERFORMING ORGANIZATION REPORT NUMBER</b>	
<b>9. SPONSORING/MONITORING AGENCY NAME(S) AND ADDRESS(ES)</b> AOARD UNIT 45002 APO AP 96338-5002				<b>10. SPONSOR/MONITOR'S ACRONYM(S)</b> AFRL/AFOSR IOA	
				<b>11. SPONSOR/MONITOR'S REPORT NUMBER(S)</b> AFRL-AFOSR-JP-TR-2019-0053	
<b>12. DISTRIBUTION/AVAILABILITY STATEMENT</b> A DISTRIBUTION UNLIMITED: PB Public Release					
<b>13. SUPPLEMENTARY NOTES</b>					
<b>14. ABSTRACT</b> The PI has successfully completed the research project. A new hydrophobic ionic liquid ferrofluid was synthesized considering potential applications under no atmosphere and in high temperature conditions. The polymer, which stabilizes the nanoparticles in the ionic liquid, can be designed to obtain the desired level of steric repulsion between particles using the predictions from the DLVO theory. The binding strength of the polymer to the nanoparticles can also be adjusted by selecting appropriate polymer blocks with multiple anchoring points. The magnetorheological behavior of the new hydrophobic ILFF evidenced that the AA10-DEAm60 diblock stabilizes the nanoparticles against aggregation of particles arising due to magnetic dipole-dipole attractive forces. Increasing the applied magnetic field strength and particle concentration in the IL increased the elastic modulus, which is a useful property for applications involving variable force fields. The shear thinning nature of the ferrofluid makes it a suitable candidate for applications involving pumping and spaying. Calculations revealed that the length of the DEAm60 segment of the polymer gave a sufficiently large steric repulsion against localized thickening of the ILFF under high shear forces. The relaxation behavior of the ferrofluid and methods to control the relaxation should be studied to use the ferrofluid in engineering applications such as electrospaying from magnetic ferrofluid spikes. There was one peer reviewed paper submitted as a direct result of the grant award.					
<b>15. SUBJECT TERMS</b> electrospray, satellite propulsion, ionic liquid ferrofluid, AOARD					
<b>16. SECURITY CLASSIFICATION OF:</b>			<b>17. LIMITATION OF ABSTRACT</b>  SAR	<b>18. NUMBER OF PAGES</b>	<b>19a. NAME OF RESPONSIBLE PERSON</b> CHEN, JERMONT
<b>a. REPORT</b>  Unclassified	<b>b. ABSTRACT</b>  Unclassified	<b>c. THIS PAGE</b>  Unclassified			<b>19b. TELEPHONE NUMBER (Include area code)</b> 315-227-7007

# Properties of ionic liquid ferrofluids

## Steric Stabilization of $\gamma$ -Fe<sub>2</sub>O<sub>3</sub> Superparamagnetic Nanoparticles in a Hydrophobic Ionic Liquid and the Magnetorheological Behavior of the Ferrofluid

Pramith Priyananda, Hadi Sabouri, Nirmesh Jain and Brian S. Hawkett\*

University of Sydney, NSW, 2006, Australia

\*Corresponding author

### ABSTRACT

Hydrophobic ionic liquid ferrofluids (ILFFs) are studied for use in electrospray thrusters for microsatellite propulsion under no atmosphere and in high temperature environments. We synthesized a hydrophobic ILFF by dispersing sterically stabilized  $\gamma$ -Fe<sub>2</sub>O<sub>3</sub> nanoparticles in the ionic liquid EMIM-NTf<sub>2</sub>. A diblock copolymer, C4-RAFT-AA<sub>10</sub>-DEAm<sub>60</sub>, was synthesized to facilitate multipoint bidentate anchoring to the nanoparticle through the acrylic acid block. The DEAm<sub>60</sub> layer was incorporated to generate steric repulsion between particles to protect against the aggregation of magnetized particles arising from dipole-dipole attraction. The effect of shearing and variation in the magnetic field strength on the steric repulsion was examined using the DLVO theory. The effect of varying the magnetic field strength and particle concentration on the viscoelastic properties of the ferrofluid was evaluated using rheometry.

The viscosity of the ferrofluid increased with the magnetic field strength, indicating the magnetized particles assembled into a structure. The level of straining required to breakdown the structure formed by the magnetized particles increased with the magnetic field strength and particle concentration. The absence of particle interlocking during shearing was indicated by the smooth viscosity vs shear rate traces. The DLVO analysis showed that increasing the magnetic attraction between the particles causes the DEAm<sub>60</sub> brush layers on the particles to overlap more, resulting in an increase in the steric repulsion. As overlapping increases osmotic repulsion is caused before progressing to a strong elastic repulsion. The effect of the polymer solubility and particle interaction due to hydrodynamic forces on the steric repulsion were also analyzed.

**Keywords:** steric stabilization, DLVO, magnetorheology, superparamagnetic, ionic liquid, ferrofluid.

### INTRODUCTION

Ferrofluids that are made up of superparamagnetic nanoparticles can change their viscosity in milliseconds in response to an applied magnetic field, and are completely demagnetized

on the removal of the applied field. This remarkable property allows engineers who seek new smart materials to finely control the magnetic field induced rheological properties of ferrofluids using electrical circuits. The ability of a ferrofluid to quickly change its flow behavior can be used to fine tune the motion of electromechanical components such as joints in robots and prosthetic limbs. In addition, these ferrofluids have been studied for use in many novel applications including microsatellite thrusters<sup>1</sup>, controlling air pollution<sup>2</sup>, new body armor<sup>3</sup>, and in artificial hearts<sup>4</sup>. The colloidal stability and rheological properties of these ferrofluids are important in applications involving shear fields, rapid motion, and magnetic fields.

Ferrofluids that are intended for use in microsatellite thrusters and other electromechanical applications in space technology should not evaporate under non-atmospheric conditions. Considering potential applications under extreme environments including satellite propulsion and oil and gas exploration<sup>5</sup>, we synthesized a ferrofluid using the hydrophobic ionic liquid EMIM-NTf<sub>2</sub> as the carrier medium for superparamagnetic  $\gamma$ -Fe<sub>2</sub>O<sub>3</sub> nanoparticles. An amphiphilic diblock copolymer consisting of a polyacrylic acid (PAA) and poly(N,N-diethylacrylamide) (DEAm) block was synthesized and anchored to the nanoparticles for the effective steric stabilization of the nanoparticle in the ionic liquid (IL). The PAA block containing 10 carboxylic acid moieties anchored to the particle through multiple bidentate bonds<sup>6</sup>. The DEAm block extends outwards to prevent particle agglomeration arising from magnetic and van der Waals attractive forces. The interaction between the polymer segments in the interface of the interacting particles is an important factor that significantly influences the rheological properties<sup>7,8</sup> exhibited by nanofluids.

To the best of our knowledge, only a very limited number of research articles<sup>9-11</sup> have dealt with the preparation of hydrophobic ionic liquid ferrofluids. These studies did not focus on the analysis of the interaction energies and forces between the magnetized particles in order to explore design methods to obtain the optimum stabilization under dynamic conditions. In addition, the viscoelastic properties of these ferrofluids, including their response to varying length scale deformations under high magnetic fields and at high particle concentrations, have not been studied thoroughly. These conditions are required when large magnetically induced thrusts need to be generated using a ferrofluid, and when they are used under dynamic conditions involving high intensity shear fields.

This study focused on evaluating the required properties of the stabilizing ligands, which in this case are block copolymers, anchored to a particle to obtain optimum steric stabilization under dynamic conditions. The interaction energies and forces arising during interaction between particles were evaluated using the DLVO theory and relevant hydrodynamics. The theoretical predictions from this evaluation deliver useful insight into the parameters that can be controlled to generate steric repulsion. The influence of the ligand solubility in the ionic liquid (IL), the length and surface density of the ligand, and the level of magnetization of the nanoparticles on the steric repulsion between nanoparticles was theoretically evaluated. The predictions and the theoretical methods used in this study are useful to pre-design ionic liquid ferrofluids to suit any intended application; however, the theoretical predictions only offer approximate values due to a number of assumptions that were applied when performing the calculations. The effect of the magnetic field strength and the particle concentration on the deformation and flow behavior of the newly developed hydrophobic ILFF was experimentally studied and is discussed in this paper.

## EXPERIMENTAL SECTION

### Preparation of ferrofluid

Diethyl acrylamide (DEAm, Aldrich) monomer was passed over an inhibitor removal column (aluminium oxide, Aldrich). Acrylic acid (AA, Aldrich), 4,4'-azobis(4-cyanovaleric acid) (V-501, Wako), 1-Ethyl-3-methylimidazolium bis(trifluoromethylsulfonyl)imide (EMIM-NTf2, 99 %, IOLITEC Ionic Liquids Technologies), 1,4-dioxane (99 %, Merck), sodium hydroxide (NaOH, Aldrich), and 2-[(butylsulfanyl)carbonothioyl]sulfanylpropanoic acid (BuPAT, DuluxGroup Australia) were used as received. The aqueous dispersion of iron oxide nanoparticles with an average diameter of approximately 25 nm (see reference in the supplementary Information) was obtained from Sirtex Medical Limited (Australia). Deionized water was used in all experiments. The block copolymer, RAFT-AA<sub>10</sub>-b-DEAm<sub>60</sub>, was prepared as reported previously<sup>12</sup>; the monomers monoacryloxyethyl phosphate and acrylamide in the reported synthesis were replaced with equimolar acrylic acid and *N,N*-diethyl acrylamide, respectively, to prepare the stabilizer for the hydrophobic ionic liquid based ferrofluid. In a typical reaction, DEAm (6.662 g, 52.3 mmol), V-501 (0.024 g, 0.087 mmol), and BuPAT (0.208 g, 0.87 mmol) were added to a 100 mL round-bottomed flask containing a mixture of dioxane (15 g) and water (7.5 g). The reactive mixture was maintained at a temperature of 70 °C for 12 h under a nitrogen atmosphere before being cooled to room temperature. Acrylic acid (0.629 g, 8.7 mmol) and V-501 (0.024 g) were then added, and the reaction mixture was heated for a further 4 h at 70 °C under nitrogen. The block copolymer formed using this procedure, typically poly(AA<sub>10</sub>-b-DEAm<sub>60</sub>), was obtained as a solution with 29 % solids (Fig. 1(a)). An aqueous dispersion of the sterically stabilized nanoparticles was prepared in water as reported previously<sup>6</sup>, and the ionic liquid ferrofluid was prepared in a similar manner to that reported for the preparation of an EAN-based ionic liquid ferrofluids<sup>11</sup>. The Fe<sub>2</sub>O<sub>3</sub> particle surface binds to the polyacrylic acid<sup>6</sup> block (PAA) through multipoint bidentate coordinate bonding, as we described previously. Sterically stabilized nanoparticles dispersed in a 50:50 (w/w) water:ethanol mixture was mixed with the ionic liquid, followed by ultrasonication for 2 min. The water and ethanol were then removed by rotary evaporation.

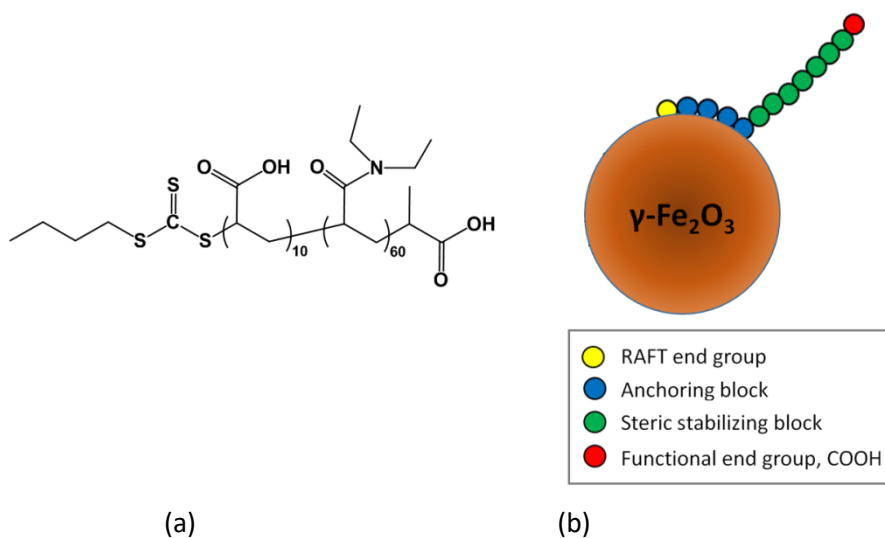


Fig.1 (a) A representative structure of the diblock copolymer (b) A schematic showing the polymer anchored to the nanoparticle. Poly acrylic acid block of the copolymer anchors on to the nanoparticle surface while the diethyl acrylamide block extends into the ionic liquid.

### **Characterization of the nanoparticles and ferrofluids**

The magnetization of the Sirtex nanoparticles was determined according to our previous publications using the vibrating sample magnetometer (VSM) method<sup>1,11</sup>. The final composition of the ferrofluid was determined by thermal gravimetric analysis (PerkinElmer Pyris 1). All samples were heated to 105 °C and equilibrated to remove residual solvent prior to analysis before being heated to 750 °C under a nitrogen atmosphere (20 mL min<sup>-1</sup>) at a rate of 20 °C min<sup>-1</sup>. The Pyris Manager software was used to calculate the weight loss.

### **Rheological testing**

Rheological testing was carried out using a Kinexus Pro (Malvern) rheometer at room temperature of 25 °C. A 1mm thick layer of the ILFF was placed on a flat plastic plate (Fig. S1). The sample was then subjected to a vertical magnetic field by placing a magnet under a thin plastic plate. Tests were carried out under different field strengths. A series of samples containing different concentrations of magnetic particles (20 to 40 % by weight) were used. The field strength was varied using a set of permanent magnets. The rotatable upper plate of the rheometer applied the pre-determined deformation to the sample. The strength of the applied magnetic field was measured using a Gauss meter (F.W. Bell Model 7010).

The response of the ferrofluid to varying length scale (amplitude sweep) deformations was studied using a 2 cm diameter parallel upper plate. An amplitude sweep was carried out in the range of 10<sup>-4</sup> to 10<sup>-1</sup> radians at a frequency of 1 Hz. The shear dependence of the viscosity was determined by gradually increasing the shearing rate.

Ferrofluid spiking was examined by placing a sample of the ferrofluid in a vertical magnetic field.

### **Modelling of interparticle interaction potential energy and forces**

The colloidal stability of the ferrofluid in the presence of a magnetic field was examined theoretically by evaluating the interparticle interaction potentials between two adjacent nanoparticles. The DLVO theory was extended to consider the potential energy due to magnetic dipole-dipole attraction and steric repulsion between the polymer-coated nanoparticles<sup>13-15</sup>. The total interaction pair potential energy was calculated by summing each interaction pair potential contribution. The pair potentials were calculated as a function of the iron oxide surface to surface separation between two nanoparticles(s) with equal diameters (25 nm). All calculations were performed using the MATLAB R11 software package.

## RESULTS AND DISCUSSION

### Characteristic properties of the ferrofluid

Magnetization curves of both the dry uncoated Sirtex nanoparticles (Sirtex NPs) and the ILFF are shown in Fig. 2. The graph shows zero hysteresis, which is a characteristic of superparamagnetism. The magnetic saturation ( $M_{\text{sat}}$ ) of the ionic liquid ferrofluid is 64.8 emu/g, which is lower than that of the bare maghemite Sirtex NPs of 70.5 emu/g.

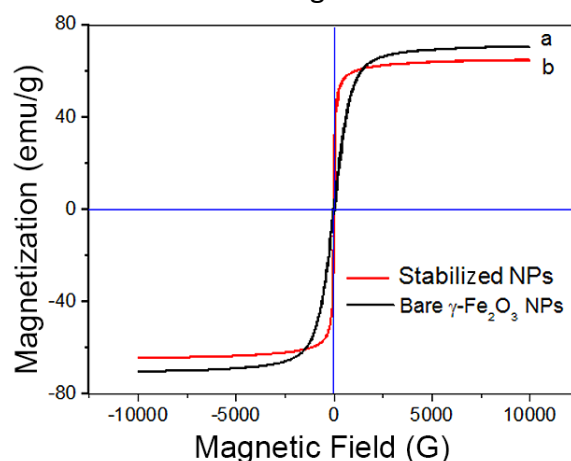


Fig. 2. Magnetization curves of the (a) Sirtex NPs in the dry state, and the (b) ionic liquid ferrofluid at room temperature.

This reduction in the magnetic saturation on anchoring the PAA block onto the maghemite particle may be due to the well-known spin canting phenomenon<sup>16</sup>. Thermal gravimetric analysis (TGA) revealed that the ionic liquid ferrofluid was thermally stable up to a temperature of 280 °C (Fig. S3). The estimated organic matter loss from the TGA trace of functionalized particles is 11g per 100 g of Fe<sub>2</sub>O<sub>3</sub> (see Fig. S2 and Fig. S3). The stability of the prepared ferrofluid at relatively high temperatures makes it a useful candidate for application under harsh environmental conditions. All ferrofluids examined with an Fe<sub>2</sub>O<sub>3</sub> concentration between 20 and 40 % (w/w) quickly spiked when a magnetic field was applied. The ability of a ferrofluid to spike upon the application of a magnetic field is essential for application in capillary free thrusters, which are being developed to propel microsattellites<sup>1</sup>.

### Colloidal stability of $\gamma$ -Fe<sub>2</sub>O<sub>3</sub> nanoparticles in EMIM-NTf<sub>2</sub>

The ferrofluid stability towards the aggregation of nanoparticles due to the attractive magnetic and van der Waals forces can be examined by calculating the interparticle interaction potential energies between a pair of nanoparticles, as mentioned in the Experimental Section. The total interaction potential can be written as:

$$V_{\text{Total}} = V_m + V_{\text{vdw}} + V_{\text{st}} + V_e \quad (1)$$

where  $V_{\text{vdw}}$ ,  $V_e$ ,  $V_m$  and  $V_{\text{st}}$  are the van der Waals, electrostatic, magnetostatic, and steric interaction potentials, and are functions of the surface-to-surface centreline separation distance ( $s$ ) between particles.

Accumulation of ion clusters at the surface of a nanoparticle can generate an electrostatic interaction potential,  $V_e$ <sup>17,18</sup>. However this electrostatic potential is negligible at the separation distance between particles that we consider in this study since the Deby length is substantially suppressed in the ionic liquid<sup>13</sup>. The van der Waals interaction potential energy was calculated according to Equation (2):<sup>13</sup>

$$V_{vdw} = -\frac{r}{12s} \left[ (\sqrt{A_1} - \sqrt{A_2})^2 \right] \quad (2)$$

where  $A_1$  and  $A_2$  are Hamaker constants of the ionic liquid and particle, respectively<sup>13,15</sup>,  $s$  is the surface-to-surface centreline separation distance between particles and  $r$  is the radius of the particle. For the calculations, the constants  $A_1$  and  $A_2$  were taken to be  $54.9 \times 10^{-21} \text{ J}$ <sup>13</sup> and  $68 \times 10^{-21} \text{ J}$ <sup>19</sup>, respectively.

The magnetostatic interaction potential energy was calculated using Equation (3):<sup>13</sup>

$$V_m = -\frac{\pi \mu_0 M^2 d^3}{9 \left( \frac{2s}{d} + 2 \right)^3} \quad (3)$$

where  $d$  is the diameter of the nanoparticles (25 nm, see Supplementary Information) used,  $\mu_0$  is the magnetic permeability of free space ( $4\pi \times 10^{-7} \text{ H.m}$ )<sup>20</sup>, and  $M$  is the magnetisation of nanoparticles.

When two particles move closer together due to magnetic attraction, the grafted polymer segments (ligands) begin to overlap, which increases the ligand concentration in this region (Fig. 3). Ligand mixing in the overlapping region causes steric repulsion. Mathematical models have been developed for well defined systems examining the action of multiple parameters that influence the steric repulsion including ligand solubility, length, surface density, particle size, and magnetization. The steric interaction potential ( $V_{st}$ ) arises due to the mixing of ligands in the overlapping region, and it has osmotic ( $V_o$ ) and elastic ( $V_{el}$ ) contributions (Equation (4))<sup>21,22</sup>. The elastic component starts to operate when the thickness of the overlapping region is less than the length of the ligand.

$$V_{st} = V_o + V_{el} \quad (4)$$

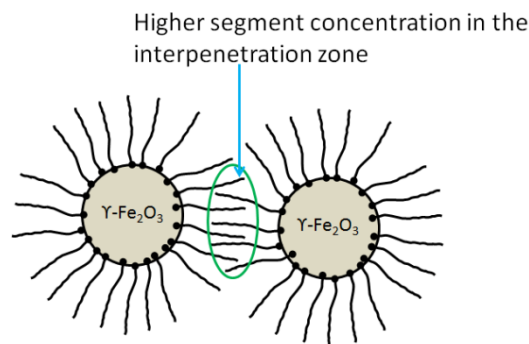


Fig. 3. Overlapping of the ligand (polymer segments) due to the magnetic attraction between two particles.

Increasing the number density of the ligand in the overlapping region causes some of the solvent molecules to be expelled into the bulk continuous phase. If the ligand is very soluble in the solvent, this exclusion of solvent molecules is thermodynamically disfavoured<sup>23</sup>. Then, competition of the solvent molecules to solvate the interpenetrating segments gives rise to the osmotic component. If the extended length of the ligand is  $l$ , and  $l < s < 2l$ , the osmotic interaction potential can be described using Equation (5) assuming that the ligand is uniformly distributed on the surface of the nanoparticle, and the nanoparticles are of equal diameter<sup>22</sup>.

$$V_o = 4\pi r k_B T N_A \frac{\varphi_p^2}{v_s} (0.5 - \chi) \left( l - \frac{s}{2} \right)^2 \quad (5)$$

where  $N_A$  is Avogadro's number,  $\chi$  is the Flory-Huggins parameter,  $\varphi_p$  is the partial specific volume of the ligand,  $r$  is the radius of nanoparticles,  $k_B$  is the Boltzmann constant and  $v_s$  is the molar volume of the ionic liquid. The calculated length of the fully extended DEAm<sub>60</sub> block (ligand) is approximately 10 nm.

Equation (5) shows that the magnitude of the osmotic component ( $V_o$ ) depends on the Flory-Huggins parameter ( $\chi$ ), which is a function of the Hildebrand solubility parameters of the polymer and the ionic liquid as shown in Equation (6):<sup>13,15</sup>

$$\chi = \frac{V_{mp}}{RT} (\delta_{pol} - \delta_{IL})^2 \quad (6)$$

$V_{mp}$  is the molar volume of the polymer,  $\delta_{pol}$  is the Hildebrand solubility parameter of the polymer and  $\delta_{IL}$  is the solubility parameter of the ionic liquid (22.31/ MPa<sup>0.5</sup>)<sup>24</sup>,  $R$  is the gas constant,  $T$  is temperature (K). The Hildebrand solubility parameter ( $\delta$ ) is defined as the square root of the cohesive energy density:<sup>25</sup>

$$\delta = \left( \frac{E_v - RT}{V_m} \right)^{\frac{1}{2}} \quad (7)$$

where  $E_v$  is the energy of vapourisation at zero pressure and  $V_m$  is the molar volume<sup>25</sup>. The cohesive energy and the molar volume of the ligand were estimated according to the group contribution method proposed by Fedros<sup>26</sup>. The estimated solubility parameter of the ligand is 20.63 MPa<sup>0.5</sup>. The calculated molar volume is  $6.99 \times 10^{-3}$  m<sup>3</sup>/mol. These values were used to calculate the Flory- interaction parameter according to Equation (6), and the calculated value is 0.008. The Flory parameter must be less than 0.5 for the ligand to dissolve well in the IL and to fully extend from the particle surface<sup>23</sup>. A small Flory parameter indicates that the ligand is very soluble in the IL, which Uke et al.<sup>27</sup> also observed.

The total interaction potential ( $V_{total} = V_m + V_{vdw} + V_{st}$ ) was also calculated when  $l < s < 2l$ . The osmotic component of the steric repulsion was calculated using Equation (5). The elastic component of the steric interaction and the van der Waals interaction potential are zero when  $s > l$  because the separation distance between the particles is too long for those interactions to start. The level of magnetization of the nanoparticles depends on the applied magnetic field. In order to examine the effect of individual components of the  $V_{tot}$  initially we chose the magnetization ( $M$ ) = 60 emu/g, which is the level of magnetization of the

ligand grafted  $\text{Fe}_2\text{O}_3$  nanoparticles in the ionic liquid at an applied external magnetic field of 1kG.

The calculated interaction potentials( $V$ ) are shown in Fig. 4(a) and Fig. 4(b).

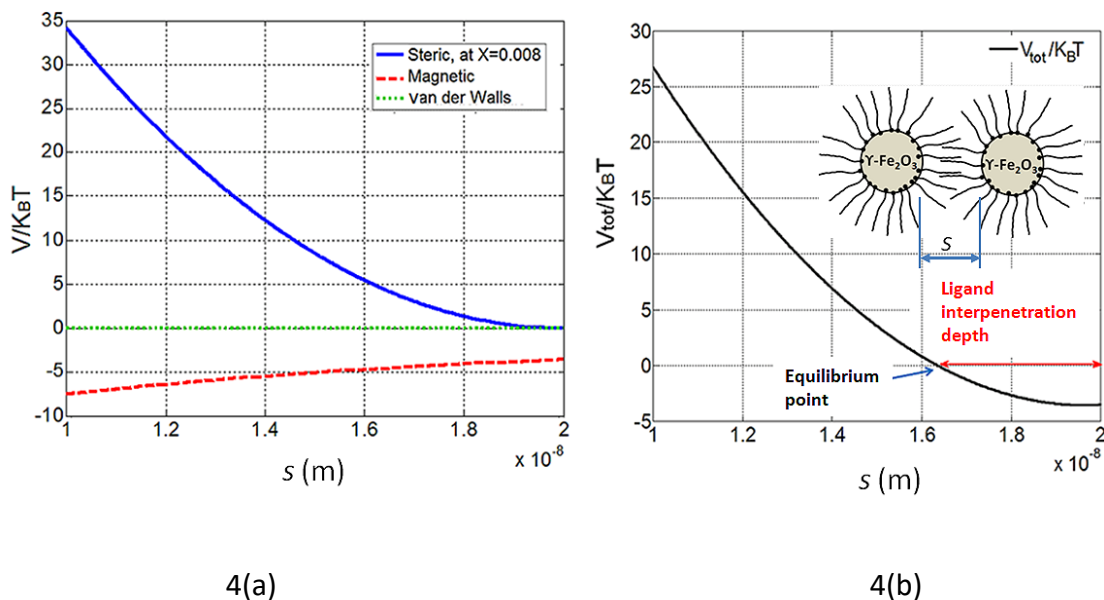


Fig. 4(a) shows individual components (steric, magnetic and van der Waals) of the interaction potentials ( $V$ ) when the magnetization,  $M$  is 60 emu/g, and 4(b) shows the net interaction potential and the depth of ligand interpenetration caused by the attractive forces between the particles.  $K_B T$  is thermal units.

The interpenetration of ligand is caused by the magnetic attraction between the nanoparticles. We examined the variation of the ligand interpenetration distance with change in the level of magnetization in the following section.

### The effect of the nanoparticle magnetization level on the ligand interpenetration

The effect of increasing the induced magnetization of the nanoparticles was examined by calculating the required ligand interpenetration depth to balance the attractive and repulsive forces. The result is shown graphically in Fig. 5.

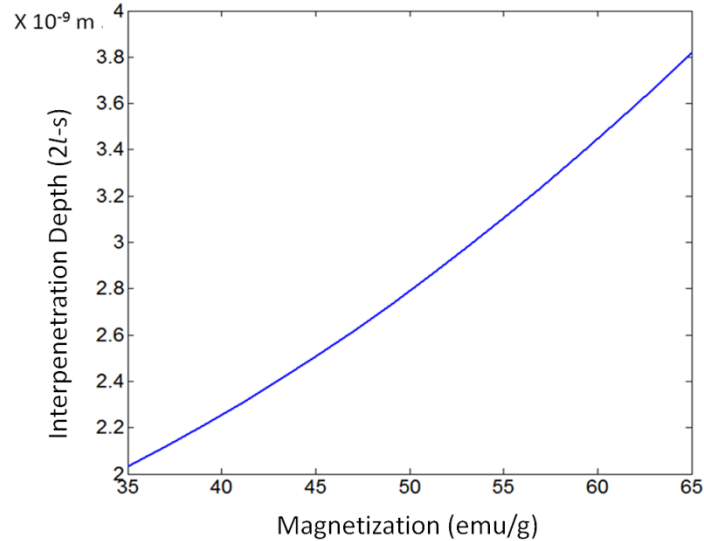


Fig. 5. Depth of interpenetration of the ligand with change in magnetization of the nanoparticles.  $l$  = the extended length of the ligand(10 nm).

As the magnetization increased, the ligand interpenetration distance also increased due to increased magnetic attraction between particles. The thickness of the ligand interpenetration or overlapping region can profoundly influence the rheological properties of any sterically stabilised colloidal system since the interpenetration of the ligand increases the segment concentration between particles, which can give rise an increase in viscosity<sup>8</sup>. We will further discuss effect of magnetic field on the viscosity of the ILFF in relation to Fig. 9 in the experimental section.

The ligand interpenetration depth can be reduced by increasing steric repulsion. According to Equation (5), steric repulsion can be increased by minimising the Flory-Huggins parameter ( $\chi$ ). Therefore, the interpenetration depth can be reduced by selecting a ligand and matching ionic liquid to obtain the minimum possible  $\chi$ . In order to explore the effect of the Flory-Huggins parameter on the ligand interpenetration depth, a hypothetical steric repulsive curve was generated by varying  $\chi$  whilst the level of magnetization was maintained at 65 emu/g (Fig. 6).

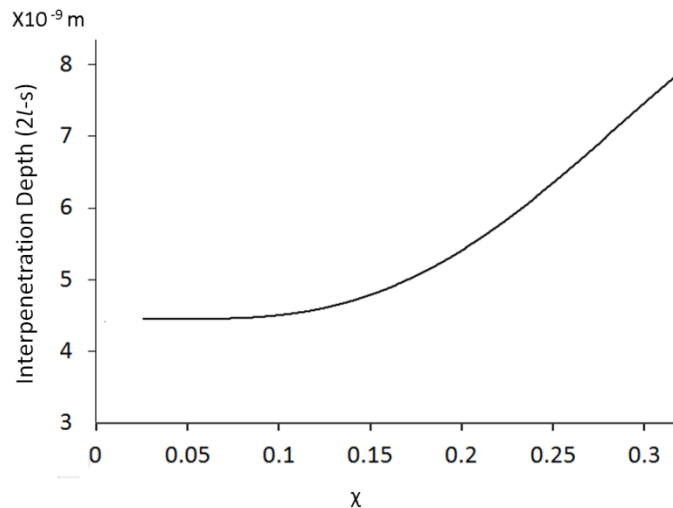


Fig. 6. Effect of changing the Flory-Huggins parameter ( $\chi$ ) on the ligand interpenetration depth.  $l$  = the extended length of the ligand(10 nm).

When Flory parameter increases, i.e., when the solvent quality decreases, a longer interpenetration depth is required to generate the required osmotic pressure to counterbalance the magnetic attraction. This calculation indicates that a change in the solubility parameters, which can occur due to a change in temperature, can profoundly affect the steric interaction potential. Also it shows the importance of choosing the matching solvent and predesigning of the ligand to obtain the desired solubility parameter to minimize the Flory-Huggins parameter. In this way we can maximize steric repulsion between the nonparticles.

On the other hand, if the nanofluid is used under very dynamic conditions such as high frequency vibration damping and pumping through piping systems where the water hammer effect can occur<sup>28</sup>, intensive and localized hydrodynamic forces can act on the particles to cause one particle to push against another particle. In this situation, the distance separating a pair of nanoparticles needs to be considered. When  $s < l$ , the ligands anchored to one particle will interact with the core of the other nanoparticle. In this case, the resulting elastic deformation of the ligand also contributes to the osmotic component of the steric interaction in addition to generating a separate elastic component. The modified osmotic potential term ( $V_{om}$ ), which accounts for the elastic deformation of the ligand, is given by:<sup>21,22</sup>

$$V_{om} = 4\pi r k_B T N_A \frac{\varphi_p^2}{v_s} (0.5 - \chi) \left[ l^2 \left( \frac{s}{2l} - \frac{1}{4} - \ln \left( \frac{s}{l} \right) \right) \right] \quad (8)$$

where

$l$  is the thickness of the grafted polymer layer,  $N_A$  is Avogadro's number,  $\chi$  is the Flory-parameter,  $\varphi_p$  is the partial specific volume of the ligand,  $v_s$  is the molar volume of the ionic liquid, and  $s < l$ <sup>21,29</sup>. The elastic repulsive component, which is analogous to a spring effect, arising due to compression of the ligand between two particles under this condition is given by:<sup>21</sup>

$$V_{el} = \frac{2\pi r k_B T N_A l^2 \varphi_p \rho}{MW_2} \left\{ \frac{s}{l} \ln \left[ \frac{s}{l} \left( \frac{3-s/l}{2} \right)^2 \right] - 6 \ln \left( \frac{3-s/l}{2} \right) + 3(1 - s/l) \right\} \quad (9)$$

where  $\rho$  and  $MW_2$  are the density and molecular weight of the ligand, respectively. The total steric interaction component when  $s < l$  is  $V_{om} + V_{el}$ . Fig. 9 shows the calculated interaction potentials ( $V_{st}$ ,  $V_{vdw}$  and  $V_m$ ) if a particle is pushing against another particle due to an external force, resulting in the reduction of  $s$  to less than  $l$ .

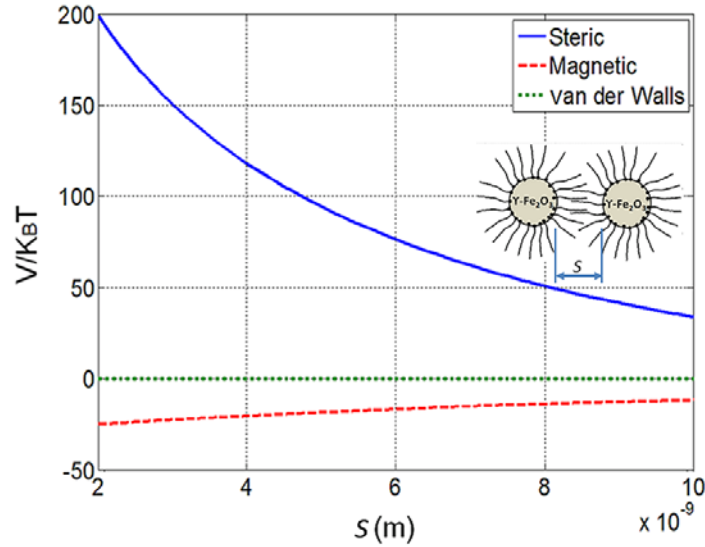


Fig. 7. The components of the total interaction potential when  $s < l$  at a magnetisation of 65 emu/g.

As shown in Fig. 7, the steric interaction potential is much larger than the magnetic and van der Waals interaction potentials when  $s < l$ . Under intensive dynamic conditions, which can be generated during damping of vibrations and impulses (e.g., body armor), the steric repulsion between particles required is larger to ensure the rapid relaxation of magnetorheological fluids. Analysis of the repulsive forces generated by steric interactions in the region where  $s < l$  provides insight into how to better target and design ferrofluids to suit such applications.

For this analysis, it is convenient to consider forces acting between a pair of particles. Assuming the motion of one particle is restricted by a possible backflow during the pressure fluctuations or formation of shear thickened regions for example, we can compare the hydrodynamic force and the steric repulsive force acting on the particles. This hydrodynamic force is given by Equation (10):<sup>30</sup>

$$F_{hyd} = 6\pi\eta r^2 \dot{\gamma} \quad (10)$$

where  $\eta$  is the viscosity of the medium (IL) of 38.6 mPa.s<sup>31</sup>,  $r$  is the radius of the particle (25 nm), and  $\dot{\gamma}$  is the local shear rate<sup>30</sup>.

The steric repulsion force, which opposes the hydrodynamic force, can be determined by differentiating the steric interaction potential with respect to the separation distance ( $s$ ). The total steric repulsion force ( $F_{st}$ ) is  $\frac{d(V_{om}+V_{el})}{ds}$ , which was calculated by differentiating Equations (8) and (9).

The surface-to-surface separation between a pair of particles when the steric repulsive force is balanced by the hydrodynamic force is shown in Fig. 8 as a function of the shear rate, which generates the hydrodynamic force. This calculation reveals that a shear rate of at least  $1.45 \times 10^5 \text{ s}^{-1}$  is required to generate a sufficiently large hydrodynamic force to balance the initial steric force, consisting of elastic and osmotic components, as the particle separation distance ( $s$ ) becomes smaller than  $l$  (Fig. 8).

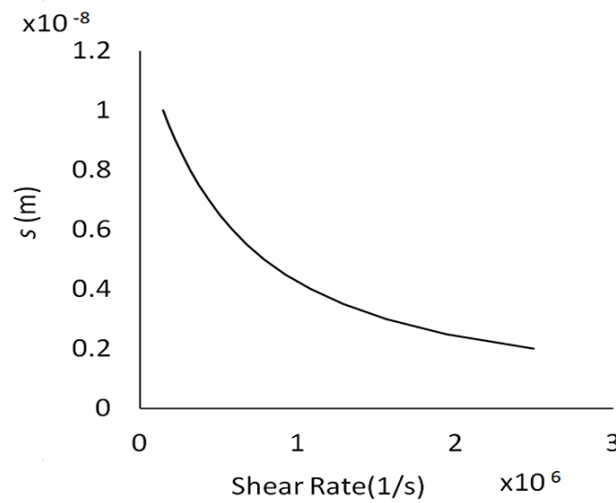


Fig. 8. Particle surface-to-surface separation distance ( $s$ ) when the hydrodynamic and steric forces are at equilibrium vs the shear rate.

### Change in rheological properties with shear rate and magnetic field

Viscosity vs shear rate traces of the ferrofluid showed that at low shear rates the viscosity can be very large depending on the applied magnetic field (Fig. 9). As the shear rate increases, the viscosity rapidly decreases, and the ferrofluid starts behaving like a Newtonian fluid.

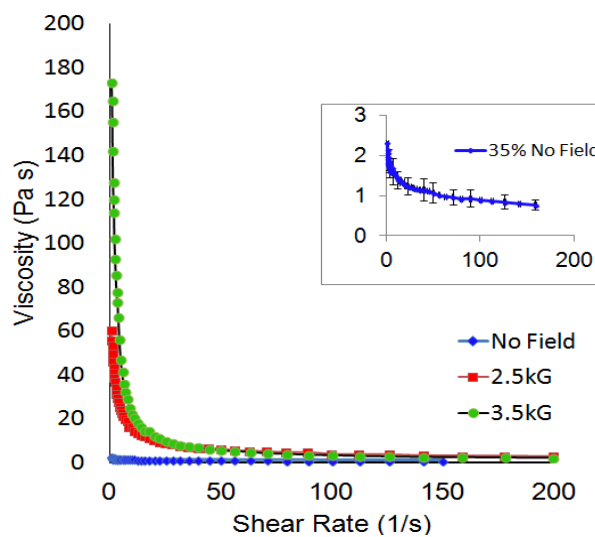


Fig. 9. Change in viscosity with shear rate and magnetic field for the ILFF containing 35 % (w/w)  $\gamma$ - $\text{Fe}_2\text{O}_3$  nanoparticles.

The large increase in viscosity with magnetic field strength at low shear rates indicates the formation of structures by the magnetized particles. Recent research on the structure of ferrofluids in magnetic fields has revealed that the nanoparticles form chains that are parallel to the magnetic field lines. This rapid assembly of nanoparticles into chains upon the

application of a magnetic field causes a rapid change in the observed rheological properties<sup>32,33</sup>.

Increase in magnetic attraction between particles should increase the interpenetration depth of ligands leading to increase in viscosity<sup>8</sup> as discussed earlier. In addition to ligand interpenetration, the increased attraction between particles make longer magnetic chains in the ferrofluid. Odenbach<sup>34</sup> discussed that the formation of stable chains increases the shear dependent viscosity. Details of this model can be found in the reference 34.

The rapid decrease in viscosity as the shear rate increases is due to layering of suspended particles under shear, which is a common feature of particle suspensions if the particles are not interlocking<sup>35</sup>. No sign of the formation of shear thickened regions was detected in the viscosity traces; although the formation of such regions is common when concentrated colloidal systems are sheared<sup>36</sup>. Relatively strong steric repulsion forces between the particles must have prevented particles from interlocking. Steric repulsion can be practically fine tuned to minimize ligand interpenetration as we have already shown (Fig. 6) by matching the solubility parameters of the ligand and the solvent. We envisage that this smooth flowing and shear thinning properties of the prepared ferrofluid, and its ability to change viscosity upon the application of a magnetic field, are important to applications involving lubrication of moving components of machines and robot joints. When the ferrofluid is used in electrospray thrusters<sup>1</sup>, a strong steric repulsion between particles makes electrospraying easier.

The critical shear strain at which the magnetically induced structure breaks is important to engineering applications involving shearing a magnetized ferrofluid; they include magnetic seals and electrospraying from ferrofluid spikes. Electrospraying from ferrofluid spikes is currently being investigated with the idea of using ferrofluids for microsatellite propulsion<sup>1</sup> and in controlling air pollution<sup>2</sup>.

The level of deformation (straining) required to breakdown the structure formed by the chains of magnetic particles can be determined by using the oscillation amplitude sweep. During an amplitude sweep the amplitude of the oscillatory deformation is varied while the frequency is kept constant. The variation in the storage (elastic) modulus of the material with increasing shear strain is then examined. Contributions to elasticity (solid-like behaviour) of a viscoelastic material are signified by the storage modulus. Fig. 10 shows how the ferrofluids respond when subjected to an amplitude sweep at a frequency of 1 Hz. Ferrofluids with different particle concentrations were tested under a number of magnetic field strengths.

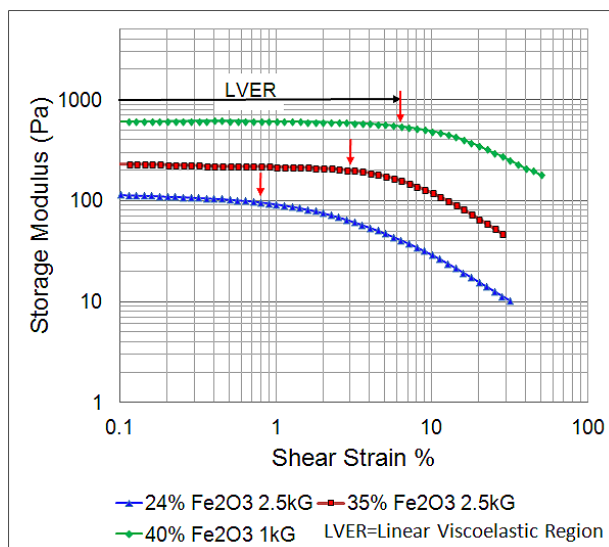


Fig. 10. Storage (Elastic) modulus of the ferrofluid containing 24 and 35 wt.%  $\text{Fe}_2\text{O}_3$  under a high magnetic field strength of 2.5 kG, and 40 wt.%  $\text{Fe}_2\text{O}_3$  under a magnetic field strength 1 kG.

Increasing both the field strength and nanoparticle concentration increased the storage modulus ( $G'$ ). When the amplitude of the deformation was gradually increased, the storage modulus remained approximately constant initially before declining after a critical strain amplitude. The period in which the storage modulus is constant is called the linear viscoelastic region (LVER), during which time the length scale deformations are not large enough to break the structure formed by the magnetic particle chains.

As soon as the storage modulus starts to decrease, the structure is disturbed. The plateau value of  $G'$  in the LVER region describes the rigidity of the sample at rest. The longer the LVER, the stronger the structure formed by the magnetized particles. As shown in Fig. 10, the higher the magnetic field strength and nanoparticle concentration, the higher the deformation (strain) required to disturb the structure formed by magnetized particles. Therefore, at a high magnetic field, a large initial deformation and thus a larger shear stress, is required to make the material flow.

## CONCLUSIONS

A new ILFF was synthesized considering potential applications under no atmosphere and in high temperature conditions. The polymer, which stabilizes the nanoparticles in the IL, can be designed to obtain the desired level of steric repulsion between particles using the predictions from the DLVO theory. The binding strength of the polymer to the nanoparticles can also be adjusted by selecting appropriate polymer blocks with multiple anchoring points. The magnetorheological behavior of the new hydrophobic ILFF evidenced that the AA<sub>10</sub>-DEAm<sub>60</sub> diblock stabilizes the nanoparticles against aggregation of particles arising due to magnetic dipole-dipole attractive forces. Increasing the applied magnetic field strength

and particle concentration in the IL increased the elastic modulus, which is a useful property for applications involving variable force fields. The shear thinning nature of the ferrofluid makes it a suitable candidate for applications involving pumping and spaying. Calculations revealed that the length of the DEAm<sub>60</sub> segment of the polymer gave a sufficiently large steric repulsion against localized thickening of the ILFF under high shear forces. The relaxation behavior of the ferrofluid and methods to control the relaxation should be studied to use the ferrofluid in engineering applications such as electrospaying from magnetic ferrofluid spikes.

## **SUPPORTING INFORMATION**

Supporting Information Available:

The set-up used for conducting rheological studies, TGA traces, and an image of ILFF spikes.

This material is available free of charge via the Internet at <http://pubs.acs.org>.

## **AUTHOR INFORMATION**

### **Corresponding Author**

E-mail: [brian.hawkett@sydney.edu.au](mailto:brian.hawkett@sydney.edu.au)

ORCID

Brian Hawkett: 0000-0001-7609-0127

### **Notes**

The authors declare no competing financial interest.

## **ACKNOWLEDGEMENTS**

This work was supported by the Asian Office of Aerospace R&D (Award NO: FA2386-16-1-4029).

## REFERENCES

- (1) King, L. B.; Meyer, E.; Hopkins, M. A.; Hawkett, B. S.; Jain, N. Self-Assembling Array of Magneto-electrostatic Jets from the Surface of a Superparamagnetic Ionic Liquid. *Langmuir* **2014**, *30*, 14143-14150.
- (2) Uehara, S.; Itoga, T.; Nishiyama, H. Discharge and Flow Characteristics using Magnetic Fluid Spikes for Air Pollution Control. *J. Phys. D: Appl. Phys.* **2015**, *48*, 282001 (5 pp).
- (3) Chiolerio, A.; Quadrelli, M. B. Smart Fluid Systems: The Advent of Autonomous Liquid Robotics. *Adv. Sci.* **2017**, *4*, 1700036.
- (4) Hahndel, T.; Stahlmann, H.-D.; Nethe, A.; Muller, J.; Buske, N.; Rehfeld, A. Ferrofluid-Supported Electromagnetic Drive for a Blood Pump for Supporting the Heart or Partially or Totally Replacing the Heart, *US Patent 6074365 A*; June 13, 2000.
- (5) Ocalan, M.; McKinley, G. H. High-Flux Magnetorheology at Elevated Temperatures. *Rheol. Acta* **2013**, *52*, 623-641.
- (6) Jain, N.; Wang, Y.; Jones, S. K.; Hawkett, B. S.; Warr, G. G. Optimized Steric Stabilization of Aqueous Ferrofluids and Magnetic Nanoparticles. *Langmuir* **2009**, *26*, 4465-4472.
- (7) Zaman, A. A.; Delorme, N. Effect of Polymer Bridging on Rheological Properties of Dispersions of Charged Silica Particles in the Presence of Low-Molecular-Weight Physically Adsorbed Poly (Ethylene Oxide). *Rheol. Acta* **2002**, *41*, 408-417.
- (8) Srivastava, S.; Shin, J. H.; Archer, L. A. Structure and Rheology of Nanoparticle–Polymer Suspensions. *Soft Matter* **2012**, *8*, 4097-4108.
- (9) Mestrom, L.; Lenders, J. J.; de Groot, R.; Hooghoudt, T.; Sommerdijk, N. A.; Artigas, M. V. Stable Ferrofluids of Magnetite Nanoparticles in Hydrophobic Ionic Liquids. *Nanotechnology* **2015**, *26*, 285602.
- (10) Medeiros, A. M.; Parize, A. L.; Oliveira, V. M.; Neto, B. A.; Bakuzis, A. F.; Sousa, M. H.; Rossi, L. M.; Rubim, J. C. Magnetic Ionic Liquids Produced by the Dispersion of Magnetic Nanoparticles in 1-n-Butyl-3-methylimidazolium bis (Trifluoromethanesulfonyl) imide (BMI. NTf<sub>2</sub>). *ACS Appl. Mater. Interfaces* **2012**, *4*, 5458-5465.
- (11) Jain, N.; Zhang, X.; Hawkett, B. S.; Warr, G. G. Stable and Water-Tolerant Ionic Liquid Ferrofluids. *ACS Appl. Mater. Interfaces* **2011**, *3*, 662-667.
- (12) Bryce, N. S.; Pham, B. T.; Fong, N. W.; Jain, N.; Pan, E. H.; Whan, R. M.; Hambley, T. W.; Hawkett, B. S. The Composition and End-Group Functionality of Sterically Stabilized Nanoparticles Enhances the Effectiveness of co-Administered Cytotoxins. *Biomater. Sci.* **2013**, *1*, 1260-1272.

- (13) Ueno, K.; Inaba, A.; Kondoh, M.; Watanabe, M. Colloidal Stability of Bare and Polymer-Grafted Silica Nanoparticles in Ionic Liquids. *Langmuir* **2008**, *24*, 5253-5259.
- (14) Worthen, A. J.; Tran, V.; Cornell, K. A.; Truskett, T. M.; Johnston, K. P., Steric Stabilization of Nanoparticles with Grafted Low Molecular Weight Ligands in Highly Concentrated Brines Including Divalent Ions. *Soft Matter* **2016**, *12* (7), 2025-2039.
- (15) Lu, H.; Du, S. A Phenomenological Thermodynamic Model for the Chemo-Responsive Shape Memory Effect in Polymers Based on Flory– Solution Theory. *Polym. Chem.* **2014**, *5*, 1155-1162.
- (16) Daou, T.; Greneche, J. Pourroy, G.; Buathong, S.; Derory, A.; Ulhaq-Bouillet, C.; Donnio, B.; Guillon, D.; Begin-Colin, S. Coupling Agent Effect on Magnetic Properties of Functionalized Magnetite-Based Nanoparticles. *Chem. Mater.* **2008**, *20*, 5869-5875.
- (17) Dupont, J.; Scholten, J. D. On the Structural and Surface Properties of Transition-Metal Nanoparticles in Ionic Liquids. *Chem. Soc. Rev.* **2010**, *39*, 1780-1804.
- (18) He, Z.; Alexandridis, P. Nanoparticles in Ionic Liquids: Interactions and Organization. *Phys. Chem. Chem. Phys.* **2015**, *17*, 18238-18261.
- (19) Faure, B.; Salazar-Alvarez, G.; Bergström, L. Hamaker Constants of Iron Oxide Nanoparticles. *Langmuir* **2011**, *27*, 8659-8664.
- (20) Rosensweig, R. E. Magnetic Fluids. *Annu. Rev. Fluid Mech.* **1987**, *19*, 437-461.
- (21) Wijenayaka, L. A.; Ivanov, M. R.; Cheatum, C. M.; Haes, A. J. Improved Parametrization for Extended Derjaguin, Landau, Verwey, and Overbeek Predictions of Functionalized Gold Nanosphere Stability. *J. Phys. Chem. C*, **2015**, *119*, 10064-10075.
- (22) Vincent, B.; Edwards, J.; Emmett, S.; Jones, A. Depletion Flocculation in Dispersions of Sterically-Stabilised Particles (“Soft Spheres”). *Colloids Surf.* **1986**, *18*, 261-281.
- (23) Napper, D. H. *Polymeric Stabilization of Colloidal Dispersions*; Academic Pr.: London, 1983; pp 200-203.
- (24) Marciniak, A. The Solubility Parameters of Ionic Liquids. *Int. J. Mol. Sci.* **2010**, *11*, 1973-1990.
- (25) Miller-Chou, B. A.; Koenig, J. L. A Review of Polymer Dissolution. *Prog. Polym. Sci.* **2003**, *28*, 1223-1270.
- (26) Fedors, R. F. A Method for Estimating Both the Solubility Parameters and Molar Volumes of Liquids. *Polym. Eng. Sci.* **1974**, *14*, 147-154.
- (27) Ueki, T.; Watanabe, M. Polymers in Ionic Liquids: Dawn of Neoteric Solvents and Innovative Materials. *Bull. Chem. Soc. Jpn.* **2011**, *85*, 33-50.

- (28) Ghidaoui, M. S.; Zhao, M.; McInnis, D. A.; Axworthy, D. H. A Review of Water Hammer Theory and Practice. *Appl. Mech. Rev.* **2005**, *58*, 49.
- (29) Saunders, S. R.; Eden, M. R.; Roberts, C. B. Modeling the Precipitation of Polydisperse Nanoparticles using a Total Interaction Energy Model. *J. Phys. Chem. C* **2011**, *115*, 4603-4610.
- (30) Nogi, K.; Hosokawa, M.; Naito, M.; Yokoyama, T.: *Nanoparticle Technology Handbook*, Second Edition, Elsevier: Amsterdam, 2012; p.165.
- (31) Fröba, A. P.; Kremer, H.; Leipertz, A. Density, Refractive Index, Interfacial Tension, and Viscosity of Ionic Liquids [EMIM][EtSO<sub>4</sub>],[EMIM][NTf<sub>2</sub>],[EMIM][N(CN)<sub>2</sub>], and [OMA][NTf<sub>2</sub>] in Dependence on Temperature at Atmospheric Pressure. *J. Phys. Chem. B* **2008**, *112*, 12420-12430.
- (32) Felicia, L. J.; Philip, J. Probing of Field-Induced Structures and Their Dynamics in Ferrofluids using Oscillatory Rheology. *Langmuir* **2014**, *30*, 12171-12179.
- (33) Furst, E. M.; Gast, A. P. Dynamics and Lateral Interactions of Dipolar Chains. *Phys. Rev. E* **2000**, *62*, 6916.
- (34) Odenbach, S., *Magnetoviscous Effects in Ferrofluids*. Springer: Berlin, 2002.pp. 80-82.
- (35) Xu, X.; Rice, S. A.; Dinner, A. R. Relation Between Ordering and Shear Thinning in Colloidal Suspensions. *Proc. Natl. Acad. Sci.* **2013**, *110*, 3771-3776.
- (36) Brown, E.; Forman, N. A.; Orellana, C. S.; Zhang, H.; Maynor, B. W.; Betts, D. E.; DeSimone, J. M.; Jaeger, H. M. Generality of Shear Thickening in Dense Suspensions. *Nat. Mater.* **2010**, *9*, 220-224.

## Table of contents graphic

